Nanoscale

View Online
Dynamic Article Links

Cite this: *Nanoscale*, 2011, **3**, 1756

www.rsc.org/nanoscale

PAPER

Mesoporous silica-coated gold nanorods: towards sensitive colorimetric sensing of ascorbic acid *via* target-induced silver overcoating

Guoqing Wang,†‡ Zhaopeng Chen† and Lingxin Chen*

Received 14th November 2010, Accepted 10th January 2011
DOI: 10.1039/c0nr00863j

This article describes a nonaggregation-based colorimetric assay of ascorbic acid by tailoring the optical properties of mesoporous silica-coated gold nanorods (MS GNRs) *via* silver overcoating. The colorimetric measurement of ascorbic acid (AA) concentration strongly relies on the fact that the blue shift effect of localized surface plasmon resonance (LSPR) peak of MS GNRs is gradually enlarged with the increase of AA amount. The limit of detection is determined to be 49 nM, which is comparable to that of quantum dots (QDs)-based fluorimetric methods.

Introduction

Ascorbic acid (AA), also called vitamin C, extensively exists in plants, animal tissues and foodstuffs, and is an essential biomolecule playing numerous roles, such as anti-oxidant, enzyme cofactor, nutritional factor and involvement in neurotransmitter-related enzymes.[1] Accordingly, it is important to develop a simple and efficient method to sensitively detect AA for various fields of study, for which purpose great research efforts have been made. The well-established approaches include titrimetric,[2] fluorometric,[3] electroanalytical,[4] chemiluminometric[5] and chromatographic methods,[6] however, they usually require sophisticated process or long detection time, making them inapplicable for simple and fast AA analysis.

Rapid and cost-effective colorimetric detection provides novel opportunities for modern bioanalysis and environmental monitoring. Over the past few years, the metal nanoparticle aggregation based-method has been one of the key research drivers in the current atmosphere of colorimetric assays. Owing to their featured localized surface plasmon resonance (LSPR) absorption and high extinction coefficient, in particular, gold nanoparticles (AuNPs) are routinely employed as colorimetric indicators.[7] Their surface functionalization with recognition elements is further shown to allow target-programmed AuNP aggregation or AuNP aggregate dispersion. By virtue of AuNPs' strong distance-dependent optical absorption, the resulting variation of absorption/color would lead to the detection of a target in a simple colorimetric or visual manner. However, the sub-stable bared AuNPs and nanoaggregates involved in these assays often give birth to non-recurring output signals. What's more, this approach requires time-consuming and fine labelling, preventing many researchers from creating their own sensing systems.

Fortunately, recent advancements in controlling surface chemistry of nanoparticles have led to a generation of non-aggregation-based colorimetric detection format relying on the chemical redox taking place on nanoparticle surfaces.[8] For instance, Chen *et al.* has devised a mercaptoethanol/$S_2O_3^{2-}$AuNPs probing system for colorimetric Pb^{2+} ion assay based upon the leaching of AuNPs, and thus their dramatic decrease in the LSPR absorption.[8c] This method holds high sensitivity and selectivity toward Pb^{2+}, and the linear detection range was over nearly 4 orders of magnitude. Recently, we have reported the colorimetric sensing of Hg^{2+} and S^{2-} with mesoporous silica-coated gold nanorods (MS GNRs) enabled by their chemical redox-modulated LSPR absorption.[9] Compared to the AuNPs applied for Pb^{2+} analysis aforementioned, the MS GNRs afford both rapid and sensitive detection of the target ions, mainly owing to the improved surface properties of the mesoporous shell,[10] and also the high sensitivity of the nanorods to the refractive index of surrounding medium.[11] To demonstrate the general applicability of our strategy and extend the use of this novel nanocomposite, we further attempted to analyze AA in a colorimetric fashion. As a reducing agent, AA may serve directly for its detection using a chemical redox approach. In the present work, we accomplish the sensitive colorimetric and visual detection of AA through the target-triggered silver overcoating of MS GNRs in the presence of Ag^+. The resulting LSPR absorption band of MS GNRs is observed to exhibit regular blueshift behavior with increasing amount of AA. A very good linear dependence between the peak shift and AA concentration is attained within a certain range, and the limit of detection is determined to be 49 nM. We expect that this new colorimetric AA sensor will find its practical applications in future food and biological analysis.

Key Laboratory of Coastal Zone Environmental Processes, CAS, Shandong Provincial Key Laboratory of Coastal Zone Environmental Processes, Yantai Institute of Coastal Zone Research, Chinese Academy of Sciences, Yantai, 264003, China. E-mail: lxchen@yic.ac.cn; Fax: (+86) 535-2109130

† Contributed equally to this work.

‡ Present address: Graduate School of Chemical Sciences and Engineering, Hokkaido University, Sapporo 001-0021, Japan.

Experimental

Cetyltrimethylammonium bromide (CTAB) was purchased from Bio Basic Int. The other chemicals were bought from Sinopharm Chemical Reagent Co., Ltd (China). All of the reagents are of analytical grade and used as received. Deionized water with 18.2 MΩ cm specific resistance was obtained from a Cascada™ LS Ultrapure water system (Pall Corp., USA), and was used for solution preparation throughout all experiments.

Transmission electron microscopy (TEM) analyses were performed on a JEM-1230 electron microscope (JEOL, Ltd., Japan) operating under 100 kV accelerating voltage. All of the absorption spectra were measured in 1 nm increments on a Beckman coulter DU-800 UV/vis spectrophotometer (USA).

MS GNRs were synthesized according to the previously reported protocols.[12] The GNR cores were first prepared by a typical seed-mediated and CTAB surfactant-directed method. In brief, 2.5 mL of CTAB (0.20 M) was mixed with 2.5 mL of $HAuCl_4$ (0.60 mM) upon stirring, to which 0.30 mL of fresh, ice-cold $NaBH_4$ solution (0.01 M) was then added. The obtained solution was stirred for another 2 min and stored as the seed solution for the next procedure. After mixing 3.75 mL of $HAuCl_4$ solution (50 mM) and 0.56 mL of $AgNO_3$ solution (50 mM) with 250 mL of CTAB solution (0.10 M) at room temperature, 3.125 mL of 0.08 M ascorbic acid (AA) was introduced with gentle stirring. Immediately, the growth solution changed from color to colorless. 0.50 mL of the seed solution was subsequently added to the growth solution at 28 °C. Then, the mixture was stirred for 10 h and the resulting colloid of GNRs was stored for further use. To achieve mesoporous silica coating, 15 mL of GNR colloidal solution was first centrifuged to remove excess CTAB molecules, and collected in 10 mL deionized water. 0.10 mL of NaOH solution (0.10 M) was then introduced to the above GNR colloid with stirring. Finally, 30 μL of 20% (m/m) Tetraethoxysilane (TOES) in methanol was added three times at a 30 min interval. The mixture was stirred for further 24 h. After the as-prepared MS GNRs were subjected to two centrifugation/wash cycles with methanol, they were finally dispersed in 10 mL of deionized water. The population of resulting GNR cores appeared to be monodisperse with an average length of 65 nm and a width of 26 nm, and the thickness of MS shells was ~8 nm. The concentration of MS GNRs was determined to be 0.68 nM assuming all gold in the $HAuCl_4$ precursor was reduced. In NaOH-Glycine buffer (50 mM, pH 9.5) system, the MS GNRs exhibit featured longitudinal and transverse LSPR absorption band centered at 663 nm and 514 nm, respectively.

For the quantitative assay of AA, 5 μL of MS GNRs and 50 μL of 10 mM Ag^+ solution were added to 395 μL of NaOH-Glycine buffer (50 mM, pH 9.5) and the resulting mixture was equilibrated for 5 min. 50 μL AA solution was then introduced and the reaction medium was left to stand for 25 min to give an optical absorption change. The absorption spectra of the AA sensing solution were collected from three independent measurements.

Results and discussion

As reported previously, the striking MS shells of MS GNRs not only help stabilize the GNRs dispersion, but also facilitate the chemical reactions on their surfaces.[9,13] Colorimetric detection of Hg^{2+} has been accomplished based on Hg^0 deposition-induced absorption change of MS GNRs in the presence of AA. It is thus reasonable to suggest that the Hg^{2+}-MS GNRs system would furnish the colorimetric assay of AA. Taking into account both the potent toxicity and hydrolysis propensity of Hg^{2+}, however, we chose Ag^+, another oxidation-active metal ion, as the appropriate component to construct the sensing system with MS GNRs for AA detection.[14] Fig. 1 shows the proposed AA sensing mechanism using our MS GNR probes, whose MS shells allow the exposure of GNR cores to the local environment to sensitively experience any dielectric change. In the presence of AA, we assumed that the chemical redox between AA and Ag^+ would generate Ag^0 catalytically depositing on the MS shells, followed by a color change of the sensing solution for colorimetric and visual detection of AA. The NaOH-Glycine system (50 mM) at pH 9.5 was used to buffer the sensing solution. On one hand, the lower pH value (pH < 9.5) is not able to endow AA with high activity. On the other hand, other species such as Ag(OH) may be formed at more alkaline environment (pH > 9.5), which is deleterious for the interaction between Ag^+ and AA.[14] Here, the concentration of Ag^+ at 1.0 mM was used to ensure the complete oxidation of AA.

To validate our speculation, we introduced 100 μM AA into the above sensing solution containing 68 pM MS GNRs, and recorded the following response of MS GNRs. The absorbance at short-wavelength region greatly increased, and both longitudinal and transverse LSPR bands of MS GNRs underwent remarkable blue shifts that reached equilibrium after 40 min, concomitant with the color change of solution from purple to green, as illustrated by the absorbance measurements and kinetic curve (Fig. 2a and Fig. 2b), respectively. The TEM images provided mechanistic insight into this interesting phenomenon. As shown in Fig. 2c, the monodisperse GNRs are encapsulated in uniform MS shells composed of disordered nanopores. After the equilibrium of reaction with AA, however, the MS shells were invisible by TEM, and a nonporous shell was observed to coat on the MS GNRs, which resulted from the MS GNRs-triggered catalytic deposition during the chemical redox. This overcoating behavior perceived by the refractive index-sensitive MS GNRs well explained our result of LSPR absorption measurements. Note that the deposition of either Hg^{2+} or Ag^+ may result in the blue shift of MS GNRs' LSPR peak, while in contrast to the Hg^0-caused absorbance decay of the MS GNRs, silver overcoating gives birth to the increased absorbance intensity.[9]

Therefore, it has been proved in principle that the MS GNRs are able to colorimetrically signal AA by taking advantage of AA-induced silver overcoating and the resulting change in MS GNRs' LSPR absorption. Nevertheless, we learned that the time

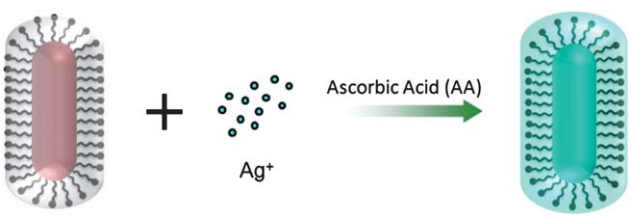

Fig. 1 Schematic representation of the LSPR sensing mechanism of AA using MS GNR probes in the presence of Ag^+.

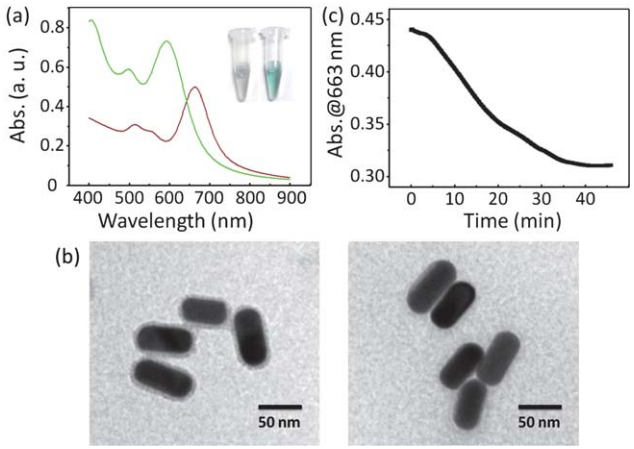

Fig. 2 (a) Absorption spectra of the MS GNRs in the absence (purple) and presence (green) of AA; the insert shows the corresponding photographs of MS GNR without (left) and with (right) AA. (b) TEM images of MS GNRs before (left) and after (right) incubation with AA. (c) Time course measurement of absorbance of MS GNRs at 663 nm after introducing AA. The final concentrations of MS GNR, Ag^+ and AA in the NaOH-Glycine buffer (pH 9.5) were 68 pM, 1.0 mM and 100 μM, respectively.

required for AA detection were relatively long for the practical application of the proposed method. To improve both detection efficiency and sensitivity of our sensing system, the MS GNRs were diluted to 6.8 pM for further investigations. We found that MS GNRs then gave a very fast colorimetric response, and the longitudinal LSPR absorption band of MS GNRs distinctly blue shifted from 663 nm to 601 nm even in the presence of 10 μM AA. The whole spectral band was observed to be greatly broadened. More importantly, the detection time was dramatically shortened to ~20 min (Fig. 3a). In order to demonstrate the application of MS GNRs for quantitative determination of AA, under the optimized conditions, we analyzed the absorption spectra of MS GNRs after incubation with AA at a series of concentrations. Regardless of the blue shift behaviors of MS GNRs at low concentration levels of AA, we only paid attention on the cases involving peak shifts larger than 2 nm, in which the concentrations of AA are above 0.1 μM. In contrast to bared GNRs associated with spurious spectral shift caused by aggregations, the absorption peak of MS GNRs is highly stable, and thus the quantification of AA using the parameter peak shift is expected to be reproducible. The absorption spectra in Fig. 3b reveals that though the MS GNRs experienced an undesired fluctuation of absorbance intensity under the AA concentration of 1.0 μM, the LSPR band displayed a steady response in the spectral shift to the increasing amount of AA throughout the range of AA concentration from 0.1 μM to 10 μM, and this shift associated with the fraction of MS GNRs bound by Ag^0 (denoted as [Ag-MS GNR]), could be used for the quantification of AA concentration. On the basis of the hypothesis that the LSPR peak shifts linearly with growing [Ag-MS GNR] and $[\text{Ag-MS GNR}]_{max} = 1$, as can be seen in Fig. 4a [Ag-MS GNR] could be plotted as a function of the concentration of AA, and followed a non-linear regression model:

$$[\text{Ag-MS GNR}] = [\text{Ag-MS GNR}]_{max} \cdot \frac{[AA]}{[AA] + K}$$

where the K is the fitting parameter and [AA] is the final concentration of AA in solution.[15] Such a non-linear fit of the data yields K = 3.145 μM. It should be pointed out that the analysis of high concentration of AA using this model may not be inclusive, since the resulting non-ideal silver deposition and Ag nanoparticles would greatly affect the peak shift behavior of the colloidal dispersion, forbidding conclusions to be made regarding cooperativity.

A very good linear response ($R^2 = 0.99$) was found in the concentration range 0.1–2.5 μM. Additionally, the limit of detection (LOD) of AA using this method was calculated to be 49 nM at a signal-to-noise ratio of 3, even lower than that (74 nM) of chemical redox-based fluorescence detection method using quantum dots (QDs).[16] We propose that the accurate analysis of AA below 0.1 μM is indeed possible by adopting smaller increments in the absorption spectrum measurement. To

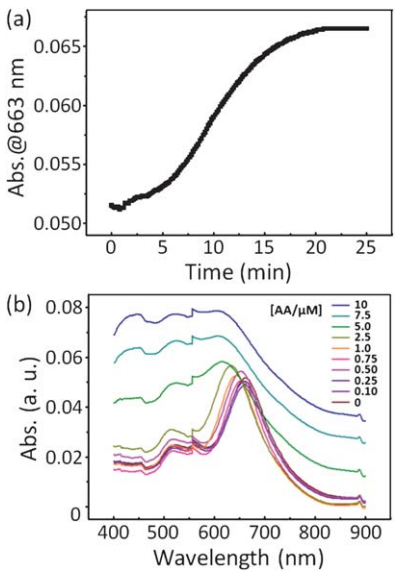

Fig. 3 (a) Time course measurement of absorbance of MS GNRs at 663 nm after introducing AA. (b) Absorption spectra of MS GNRs upon incubation with AA at various concentrations ranging from 0 to 10 μM (0, 0.10, 0.25, 0.50, 0.75, 1.0, 2.5, 5.0, 7.5 and 10 μM, respectively). The concentration of MS GNR was 6.8 pM. Other conditions were the same as those described in Fig. 2.

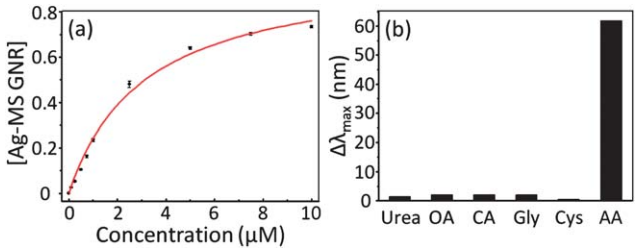

Fig. 4 (a) Variation of [Ag-MS GNRs] as a function of AA concentration. Error bars indicate the standard deviation obtained from three independent measurements. (b) Selectivity of the MS GNR nanoprobes toward AA over some other coexisting acids and compounds. The final concentrations of AA and all the interference species were 10 μM. Other conditions were the same as those described in Fig. 3.

Table 1 Comparison of analytical performances of various typical techniques for AA analysis

Method	Technique in detail	Linear range, detection limit	Assay time	Comments	Ref.
Fluorometry	FIA-fluorescence determination	0.14–2.80 μM, 0.14 μM	—	Complicated	3
Electrochemistry	HPLC-amperometric detection	10–90 μM, 90 nM	>20 min	Complicated	4*c*
Electrochemistry	Voltammetric detection using poly(l-valine) modified glassy carbon electrode	0.01–1.0 mM, 3.0 μM	—	Complicated	4*d*
Chemiluminescence	FIA-enzyme catalyzed-chemiluminometric detection	10–1000 mM, 5.0 μM	15 min	Complicated	5
Chromatography	GC–FID	0.23–11.36 mM, 0.23 mM	≥72 min	Complicated	6
Colorimetry	Cu^{+}-catalyzed alkyne–azide click reaction inducing reduction of distance among AuNPs	4.4–30 nM, 3.0 nM	20 min	Simple, aggregation-based, dual labeling	7*f*
Colorimetry	Silver overcoating inducing plasmon peak shift of MS GNRs	0.1–2.5 μM, 49 nM	20 min	Simple, non-aggregation, label-free	Present work

further assess the performance of the MS GNR nanoprobes, we tested their selectivity toward AA relative to other species, such as urea, oxalic acid (OA), citrate acid (CA), glycine (Gly) and cysteine (Cys), some of which coexist with AA in real samples. As visualized in Fig. 4b, the LSPR peak of the sensing solution responded specifically in the presence of AA, suggesting great application potential of the MS GNRs-based nanoprobes.

Conclusions

To sum up, we have communicated a new and convenient approach to colorimetric AA detection by employing MS GNRs as both recognizers and indicators. In this chemical redox-based sensing format, the MS GNRs-based LSPR probe enables rapid, sensitive and reproducible colorimetric detection. The proposed method appears to be more advantageous over other methods as shown in Table 1. This target-induced metal overcoating also illustrated a facile way to colorimetric detection by tailoring the optical properties of nanoparticles, which would be of interest for researchers of many fields.

Abbreviations

FIA	Flow injection analysis
HPLC	High performance liquid chromatography
GC	Gas chromatography
FID	Flame ionization detection
AuNPs	Gold nanoparticles
LSPR	Localized surface plasmon resonance
MS GNRs	Mesoporous silica-coated gold nanorods

Acknowledgements

We thank the financial support from the National Natural Science Foudation of China (No. 20975089), Innovation Projects of the Chinese Academy of Sciences (KZCX2-EW-206), the Department of Science and Technology of Shandong Province (No. 2008GG20005005, BS2009DX006), the Department of Science and Technology of Yantai City of China (2007156) and the 100 Talents Program of the Chinese Academy of Sciences.

Notes and references

1 (*a*) S. Padayatty, A. Katz, Y. Wang, P. Eck, O. Kwon, J. Lee, S. Chen, C. Corpe, A. Dutta, S. Dutta and M. Levine, *J. Am. Coll. Nutr.*, 2003, **22**, 18; (*b*) P. Janda, J. Weber, L. Dunsch and A. B. P. Lever, *Anal. Chem.*, 1996, **68**, 960.
2 K. K. Verma, A. Jain, B. Sahasrabuddhey, K. Gupta and S. Mishra, *J. AOAC*, 1996, **79**, 1236.
3 A. A. Ensafi and B. Rezaei, *Anal. Lett.*, 1998, **31**, 333.
4 (*a*) S. Mannino and M. S. Cosio, *Analyst*, 1997, **122**, 1153; (*b*) S. Shahrokhian and H. R. Zare-Mehrjardi, *Electroanalysis*, 2007, **21**, 2234; (*c*) Z. Gazdik, O. Zitka, J. Petrlova, W. Adam, J. Zehnalek, A. Horna, V. Reznicek, M. Beklova and R. Kizek, *Sensors*, 2008, **8**, 7097; (*d*) W. Hu, D. Sun and W. Ma, *Electroanalysis*, 2010, **22**, 584.
5 A. F. Dãnet, M. Badea and H. Y. Aboul-Enein, *Luminescence*, 2000, **15**, 305.
6 F. O. Silva, *Food Control*, 2005, **16**, 55.
7 (*a*) N. L. Rosi and C. A. Mirkin, *Chem. Rev.*, 2005, **105**, 1547; (*b*) G. Wang, Y. Wang, L. Chen and J. Choo, *Biosens. Bioelectron.*, 2010, **25**, 1859; (*c*) Z. Wang and Y. Lu, *J. Mater. Chem.*, 2009, **19**, 1788; (*d*) W. Zhao, M. A. Brook and Y. Li, *ChemBioChem*, 2008, **9**, 2363; (*e*) Y.-W. Lin, C.-W. Liu and H.-T. Chang, *Anal. Methods*, 2009, **1**, 14; (*f*) Y. Zhang, B. Li and C. Xu, *Analyst*, 2010, **135**, 1579.
8 (*a*) L. Shang and S. Dong, *Anal. Chem.*, 2009, **81**, 1465; (*b*) L. Shang, L. Jin and S. Dong, *Chem. Commun.*, 2009, 3077; (*c*) Y.-Y. Chen, H.-T. Chang, Y.-C. Shiang, Y.-L. Hung, C.-K. Chiang and C.-C. Huang, *Anal. Chem.*, 2009, **81**, 9433.
9 G. Wang, Z. Chen, W. Wang, B. Yan and L. Chen, *Analyst*, 2011, **136**, 174.
10 (*a*) J. Kim, J. E. Lee, J. Lee, J. H. Yu, B. C. Kim, K. An, Y. Hwang, C. H. Shin, J. G. Park and T. Hyeon, *J. Am. Chem. Soc.*, 2006, **128**, 688; (*b*) J. Kim, H. S. Kim, N. Lee, T. Kim, H. Kim, T. Yu, I. C. Song, W. K. Moon and T. Hyeon, *Angew. Chem., Int. Ed.*, 2008, **47**, 8438; (*c*) S. H. Joo, J. Y. Par, C.-K. Tsung, Y. Yamada, P. Yang and G. A. Somorjai, *Nat. Mater.*, 2010, **8**, 126.
11 (*a*) H. Chen, X. Kou, Z. Yang, W. Ni and J. Wang, *Langmuir*, 2008, **24**, 5233; (*b*) X. Huang, S. Neretina and M. A. EI-Sayed, *Adv. Mater.*, 2009, **21**, 1.
12 B. Nikoobakht and M. A. EI-Sayed, *Chem. Mater.*, 2003, **15**, 1957; I. Gorelikov and N. Matsuura, *Nano Lett.*, 2008, **8**, 369.
13 C. Wu and Q.-H. Xu, *Langmuir*, 2009, **25**, 9441.
14 Wuhan University, *Analytical Chemistry* (4th Ed.), 2000, Beijing: Higher Education Press. Note: $\lg(\alpha_{Hg(OH)}) = 0.5$ when pH = 3, while $\lg(a_{Ag(OH)}) = 0.1$ at pH 11, in which $\lg(\alpha_{Hg(OH)})$ and $\lg(a_{Ag(OH)})$ denote the logarithmic side reaction coefficients of Hg^{2+} and Ag^{+}, respectively. These indicate that Hg^{2+} and Ag^{+} in aqueous solution start to hydrolyze at around pH 3 and around pH 11, respectively.
15 G. Wang, C. Lim, L. Chen, H. Chon, J. Choo, J. Hong and A. J. de Mello, *Anal. Bioanal. Chem.*, 2009, **394**, 1827.
16 Y.-J. Chen and X.-P. Yan, *Small*, 2009, **5**, 2012.